Bol. Soc. Paran. Mat.
©SPM – E-ISSN-2175-1188
SPM: www.spm.uem.br/bspm

(3s.) **v. 2026 (44) 12** : 1–17.
ISSN-0037-8712
doi:10.5269/bspm.81508

Magnetohydrodynamic Natural Convection of Water-Based SWCNT and MWCNT Hybrid Nanofluid Inside a C-Shaped Cavity by Varying Aspect Ratios

Pamod S., Sujatha N., Sreekala C. K.

ABSTRACT: This research article numerically investigates the natural convection and heat transfer analysis of water-based hybrid nanofluid composed of single-walled and multi-walled carbon nanotubes inside a C-shaped cavity under the magnetic field effect. The left vertical wall of the cavity is maintained at a uniform temperature T_h, whereas a specified portion of the right wall is kept at a constant temperature T_c. The remaining sections of the cavity boundaries are assumed to be thermally insulated. The study analyses the impact of parameters such as Rayleigh number ($Ra = 10^4 - 10^7$), the Hartmann number ($Ha = 0 - 100$), the volume fraction ($\phi_{np} = 1\%$ - 4%) of the nanoparticles on the heat transfer and fluid flow within the enclosure. Additionally, the influence of aspect ratio variations ($AR = 0.25 - 0.75$) on heat transfer and fluid flow is analysed. The Galarkin's finite element method is used to solve the governing equations and the numerical solution is represented by plotting streamlines and isotherms. The results show that increasing the Rayleigh number strengthens convective motion, while higher Hartmann numbers suppress convection, causing heat transfer to be dominated by conduction. It is also notable that increasing the aspect ratio reduces the fluid flow rate due to limited space for rotation within the cavity, while smaller aspect ratios enhance thermal performance by promoting stronger fluid circulation.

Keywords: Natural convection, hybrid nanofluid, magnetohydrodynamics, Hartmann number, Rayleigh number.

Contents

1. Introduction

The study of convection has gained the substantial progress over the past century, primarily due to its broad applications in engineering and scientific domains. Natural convection, also known as free convection, happens when fluid movement is caused by buoyancy forces. These forces arise because a fluid is subjected to a body force, such as gravity, which acts on spatial variations in density within the fluid. These density variations typically a result of temperature gradients, which triggers the fluid motion and establish the convective flow patterns. This fundamental mechanism is essential in diverse applications including the design of heat ex-changers, ventilation devices, solar energy systems, atmospheric circulation, thermal regulations of water bodies etc. It also plays an pivotal role in the effective dissipation of heat from high-power electronic devices, nuclear reactors, and other thermal management technologies.

2020 *Mathematics Subject Classification:* 76D05, 76R10, 76W05.
Submitted January 23, 2026. Published April 21, 2026.

Table 1: Nomenclature

Symbol	Description	Symbol	Description
H	Height of the cavity	ρ	Density
AR	Aspect ratio	μ	Dynamic viscosity
L	$L = AR \times H$	κ	Thermal conductivity
g	Gravitational acceleration	Cp	Specific heat capacity
B_0	Magnetic field strength	β	Thermal expansion coefficient
T_m	Mean temperature	α	Thermal diffusivity, $\alpha = \frac{k}{\rho Cp}$
T_h	Hot wall temperature	σ	Electrical conductivity
T_c	Cold wall temperature	ϕ_{np}	Volume fraction
ΔT	Temperature difference	Nu	Local Nusselt number
Ra	Rayleigh number	$\bar{Nu}$	Average Nusselt number
Ha	Hartmann number		
Pr	Prandtl number		

Magnetohydrodynamic (MHD) convection arises from the coupling between an applied magnetic field and buoyancy-induced fluid motion in electrically conducting media. This interaction plays a vital role in regulating thermal transport in nuclear reactor systems, improving the efficiency of energy conversion processes in power generation technologies, and representing fluid behavior in astrophysical and geophysical flows. Moreover, the ability of magnetic fields to influence conductive fluids underpins recent developments in modern energy applications and provides an effective means for thermal control in advanced electronic and electrical devices.

Nanofluids are specially formulated heat-transfer fluids created by dispersing nanoscale particles, such as metals, carbon-based materials, or metal oxides, into conventional base liquids including water, oil, or monoethylene glycol. The presence of these nanoparticles modifies the thermo-physical behavior of the host fluid, leading to enhanced thermal conductivity and improved heat transport capability. Such improvements have enabled effective thermal management in a broad range of engineering applications, including cooling of high-power electronic devices, thermal control in automotive systems, performance enhancement of solar thermal collectors, and advanced HVAC technologies. Further advancements are achieved through hybrid nanofluids, which incorporate multiple types of nanoparticles to exploit synergistic effects, resulting in superior thermal performance, improved stability, and higher energy efficiency. Owing to these advantages, nanofluids and hybrid nanofluids are increasingly considered suitable for compact, high-performance thermal systems such as heat exchangers, automotive radiators, solar energy devices, and biomedical cooling applications.

Over the past two decades, the buoyancy - driven convection of nanofluid and hybrid nanofluid inside a $C-$ shaped cavity has been widely explored by many investigators. Due to their capacity to improve fluid circulation and heat transfer efficiency, these cavities are utilized in many engineering applications. They are suitable for use in electronic cooling systems, solar energy collectors, thermal insulation in buildings, heat exchangers, and microfluidic devices thanks to their distinctive geometry. In particularly compact or space - constrained systems, the cavity's curved structure facilitates effective passive thermal management, increases heat transfer surface area, and encourages recirculating flow.

2. Literature Survey

Natural convection heat transfer of Cu-water nanofluid inside the C-shaped enclosures was numerically investigated using the finite volume method and SIMPLER algorithm [1], revealing that heat transfer improves with increasing Rayleigh number Ra and Cu nanoparticle volume fraction ϕ_{np}, and is more significant in narrow enclosures, especially at low Rayleigh numbers. The numerical investigation of free convection of Cu-water nanofluid in a C-shaped cavity with localized heat sources [2] revealed an increase in heat transfer due to higher Ra values and Cu nanoparticle volume fractions, especially in narrow enclosures and at low Rayleigh numbers, regardless of the aspect ratio Ar. M.A.Y. Bakier [3]

numerical study revealed that in a partially C-shaped open-ended nanofluid-filled enclosure, heat transfer is significantly influenced by aspect ratio, heat source length, and nanoparticle presence, with enhanced transfer occurring at low Rayleigh numbers and optimal open region placement. Satyajit Mojumder et al. [4] numerical investigation of free convection inside a C-shaped cavity filled with cobalt-kerosene ferrofluid revealed that higher Rayleigh numbers and increased nanoparticle volume fractions enhance heat transfer, while magnetic fields suppress it. N. Makulati et al. [5] found that in an inclined C-shaped cavity with alumina–water nanofluid, heat transfer improves with aspect ratio, nanoparticle concentration, and inclination, but decreases with Hartmann number, becoming geometry insensitive at high Rayleigh numbers. Rasul Mohebbi et al. [6] showed that in a C-shaped cavity filled with nanofluid, optimal heat transfer occurs in the upper horizontal section at low Rayleigh numbers and in the upper vertical section at high Rayleigh numbers, emphasizing the impact of heat source location. By applying the Lattice Boltzmann method, Mohsen Izadi et al. [7] showed that in a C-shaped cavity, the heat source aspect ratio significantly affects heat transfer at low Rayleigh numbers ($Ra = 10^3$), while at $Ra = 10^6$, the Nusselt number increases linearly with cavity aspect ratio, indicating reduced geometric influence.

Several studies have investigated natural convection in various cavity geometries using carbon nanotube (CNT) - based nanofluids to enhance heat transfer. Mohammad Hemmat Esfe et al. [8] found that the mean Nusselt number increases with Rayleigh number in a trapezoidal enclosure using CNT - EG - water nanofluid, while Amin Matori et al. [9] showed that placing a hot obstacle at the center of a π-shaped cavity improves heat transfer with MWCNT/Fe_3O_4/water hybrid nanofluid. Dwesh K. Singh [10] reported up to 65% enhancement in the Nusselt number in rectangular cavities using MWCNT nanofluid with high CNT aspect ratios. Reza Sarlak et al. [11] observed that increasing volume fraction (ϕ) and inclination in triangular cavities boosts heat transfer but also increases viscosity and momentum dissipation. Mohsen Izadi et al. [12] used the Lattice Boltzmann Method in $\perp$-shaped enclosures and found that higher obstruction ratios reduce heat transfer, while a larger heat source aspect ratio improves cooling. Pranit Joshi, Arvind Pattamatta, and Patrice Estelle et al. [13,14] concluded that MWCNT/water nanofluids generally outperform Al_2O_3/water, though high CNT concentrations and non-Newtonian effects can lower Nusselt numbers under certain conditions.

The researchers also explored MHD natural convection in nanofluid-filled enclosures of various shapes and configurations. Rizwan Ul Haq et al. [15] examined water - based SWCNT nanofluids in partially heated C-shaped and triangular cavities, as well as through parallel fins, explored that for higher Rayleigh number and nanoparticle volume fraction there is an enhancement in heat transfer, while higher Hartmann numbers suppress it. M. Hamid et al. [16] analysed a fin-shaped cavity with a cylindrical obstacle, observing improved local Nusselt numbers with CNT addition and radiation, especially at the cavity corners. Desh Deepak Dixit and Arvind Pattamatta [17] found that the magnetic field reduces heat transfer in nanofluids mixed with MWCNTs and other nanoparticles, depending on its strength and orientation. Rizwan Ul Haq et al. [18] investigated MHD buoyancy convection of water – SWCNT nanofluid in a square chamber with parallel fins, showing improved heat transfer with increased bottom fin length. However, heat transfer decreases at higher Rayleigh numbers and nanoparticle concentrations. Oktay Cicek et al. [19] numerically investigated the hybrid nanofluid flow and found that increased volume fraction improves both heat transfer and nanoparticle deposition, especially at low Rayleigh numbers. Fatih Selimefendigil and Hakan F. Öztop [20] studied melting behavior in a corrugated cavity under inclined magnetic fields, showing that CNT addition offsets magnetic damping effects. Sardar Bilal et al. [21] examined a star-shaped cavity and found enhanced flow and Nusselt number at 5% volume fraction. T.O. Scott et al. [22] experimentally confirmed that hybrid Al_2O_3–MWCNT nanofluids significantly enhance heat transfer. Rizwan Ul Haq et al. [23] numerically studied MHD natural convection of water - SWCNT nanofluid in a triangular enclosure with a heated cylindrical obstacle, finding lower heat transfer at the heated section compared to the cold cylinder, though it improves with higher Rayleigh numbers and nanoparticle concentration. Zafar H. Khan et al. [24] investigated a partially heated trapezoidal cavity and observed that stream strength increases with Ra but diminishes with stronger magnetic fields; the highest local Nusselt numbers occur near the heating edges. L. Th. Benos et al. [25] analytically examined CNT–water nanofluid convection in a shallow cavity under internal heating and an external magnetic field, showing that increasing CNT concentration suppresses convection due to viscosity and aggregation effects. Eid S. Alatawi [26] explored MHD convection and radiation in a circular cavity with a square

obstruction, highlighting that higher Rayleigh numbers and nanoparticle volume fractions enhance heat transfer, while higher Hartmann numbers reduce it, emphasizing the importance of cavity geometry and MHD effects in thermal system performance. Rizwan Ul Haq et al. [27] investigated buoyancy - driven convection in a SWCNT nanofluid filled partially heated trapezoidal cavity using a modified thermal conductivity model and Galerkin FEM. Results showed that shorter heated lengths intensified flow, and higher Ra and nanoparticle concentrations improved heat transfer, with nanofluids outperforming base fluids. Yuan Ma et al. [28] numerically studied MWCNT–water nanofluid convection in a U-shaped enclosure with a heated obstacle using the lattice Boltzmann method. Heat transfer increased with Ra and volume fraction, peaking when the obstacle was at the bottom for high Ra (10^6) and in side channels for lower Ra (10^3–10^5), emphasizing the influence of geometry and nanofluid properties.

To date, there has been limited investigation into the magnetohydrodynamic (MHD) natural convection behavior of hybrid nanofluids within the geometries such as C-shaped cavities. This study addresses this research gap by examining the MHD natural convection of a water-based hybrid nanofluid composed of SWCNT and MWCNT inside the C-shaped cavity with varying aspect ratios. The novelty of this work lies in the simultaneous consideration of hybrid nanofluid properties, cavity geometry, and magnetic field effects, providing deeper insight into controlling heat transfer and fluid flow characteristics. The findings offer potential applications in designing more efficient cooling systems, microfluidic devices, and thermomagnetic technologies.

3. Physical Configuration

In this analysis, we consider a two-dimensional, steady, laminar, incompressible non - Newtonian hybrid nanofluid flow inside a C-shaped cavity of height $H = 1m$, aspect ratio (AR), where $L = H \times AR$ as shown in **Figure 1**. A uniform magnetic field with magnitude B_0 is imposed along the positive $x-$direction of the cavity. The left wall is kept at a constant hot temperature T_h, while part of the right wall is maintained at a cold temperature T_c. The top and bottom walls, along with a portion of the right wall, are adiabatic.The space within the enclosure is filled with a water-based hybrid nanofluid composed of single-walled carbon nanotubes (SWCNT) and multi-walled carbon nanotubes (MWCNT). All physical properties of water are assumed to be constant except for its density, which varies with temperature. This variation is accounted for by the Boussinesq approximation in the y-momentum equation. Viscous dissipation, internal heat generation, and thermal radiation effects are neglected in this study.

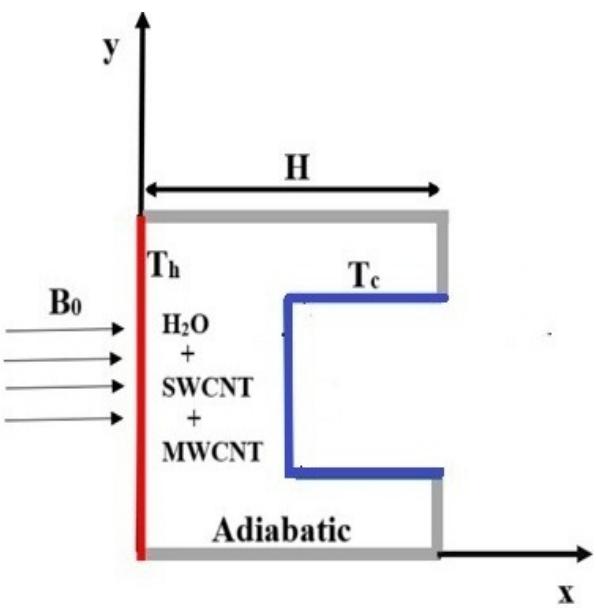

Figure 1: Physical configuration under consideration

4. Mathematical Model

Under these assumptions, the mathematical model of the problem in terms of continuity, momentum, and energy equations are [18,29,30]:

$$\frac{\partial u}{\partial x}+\frac{\partial v}{\partial y}=0. \tag{4.1}$$

$$\rho_{\text{hnf}}\left(u\frac{\partial u}{\partial x}+v\frac{\partial u}{\partial y}\right)=-\frac{\partial p}{\partial x}+\mu_{\text{hnf}}\left(\frac{\partial^2 u}{\partial x^2}+\frac{\partial^2 u}{\partial y^2}\right) \tag{4.2}$$

$$\begin{aligned}\rho_{\text{hnf}}\left(u\frac{\partial v}{\partial x}+v\frac{\partial v}{\partial y}\right)=-\frac{\partial p}{\partial y}\quad&+\mu_{\text{hnf}}\left(\frac{\partial^2 v}{\partial x^2}+\frac{\partial^2 v}{\partial y^2}\right)\\&-\sigma_{\text{hnf}}B_0^2 v+(\rho\beta)_{\text{hnf}}\,g(T-T_c)\end{aligned} \tag{4.3}$$

$$(\rho C_p)_{\text{hnf}}\left(u\frac{\partial T}{\partial x}+v\frac{\partial T}{\partial y}\right)=k_{\text{hnf}}\left(\frac{\partial^2 T}{\partial x^2}+\frac{\partial^2 T}{\partial y^2}\right) \tag{4.4}$$

The effective density, specific heat, and thermal expansion coefficient of nanoparticles and hybrid nanofluid are obtained from the following equations [29],

$$\phi=\phi_{SWCNT}+\phi_{MWCNT} \tag{4.5}$$

$$\rho_{np}=\frac{(\phi\rho)_{MWCNT}+(\phi\rho)_{SWCNT}}{\phi} \tag{4.6}$$

$$(Cp)_{np}=\frac{(\phi Cp)_{MWCNT}+(\phi Cp)_{SWCNT}}{\phi} \tag{4.7}$$

$$\beta_{np}=\frac{(\phi\beta)_{MWCNT}+(\phi\beta)_{SWCNT}}{\phi} \tag{4.8}$$

$$\kappa_{np}=\frac{(\phi\kappa)_{MWCNT}+(\phi\kappa)_{SWCNT}}{\phi} \tag{4.9}$$

$$\sigma_{np}=\frac{(\phi\sigma)_{MWCNT}+(\phi\sigma)_{SWCNT}}{\phi} \tag{4.10}$$

$$\rho_{\text{hnf}}=(1-\phi)\rho_{\text{bf}}+(\phi\rho)_{\text{np}} \tag{4.11}$$

$$(\rho C_p)_{\text{hnf}}=(1-\phi)\,(\rho C_p)_{\text{bf}}+(\phi\rho C_p)_{\text{np}} \tag{4.12}$$

$$(\rho\beta)_{\text{hnf}}=(1-\phi)\,(\rho\beta)_{\text{bf}}+(\phi\rho\beta)_{\text{np}} \tag{4.13}$$

$$\kappa_{\text{hnf}}=\kappa_{\text{bf}}\left[\frac{\kappa_{\text{np}}+2\kappa_{\text{bf}}-2\phi_{\text{np}}(\kappa_{\text{bf}}-\kappa_{\text{np}})}{\kappa_{\text{np}}+2\kappa_{\text{bf}}+\phi_{\text{np}}(\kappa_{\text{bf}}-\kappa_{\text{np}})}\right] \tag{4.14}$$

$$\sigma_{\text{hnf}}=\sigma_{\text{bf}}\left[1+\frac{3\,\phi\left(\frac{\sigma_{\text{np}}}{\sigma_{\text{bf}}}-1\right)}{\left(\frac{\sigma_{\text{np}}}{\sigma_{\text{bf}}}+2\right)-\phi\left(\frac{\sigma_{\text{np}}}{\sigma_{\text{bf}}}-1\right)}\right] \tag{4.15}$$

$$\mu_{\text{hnf}}=\frac{\mu_{\text{f}}}{(1-\phi)^{2.5}} \tag{4.16}$$

$$\Delta T=\frac{Rak_{bf}\mu_{bf}}{\rho_{bf}^2 Cp_{bf}g\beta_{bf}H^3} \tag{4.17}$$

where $T_h=T_m+0.5\Delta T$; $T_c=T_m-0.5\Delta T$;
and the subscripts bf, np and hnf respectively represent the base fluid, nanoparticle and hybrid nanofluid.

Table 2: Thermophysical properties [31] at temperature T_m=293[K].

	ρ $kg\,m^{-3}$	C_p $J\,kg^{-1}\,K^{-1}$	κ $W\,m^{-1}\,K^{-1}$	β K^{-1}	σ $S\,m^{-1}$
Water	997.1	4179	0.613	2.1×10^{-4}	0.05
SWCNT	2600	425	6600	3.3×10^{-6}	1.9×10^{-4}
MWCNT	2100	796	3000	4.2×10^{-5}	1.9×10^{-4}

Table 3: Boundary conditions for the current literature [29]

Boundary	**Wall**	**Velocity Condition**	**Thermal Condition**
Horizontal	Top($y=H$)	$u=0,\ v=0$	$\frac{\partial T}{\partial y}=0$
	Bottom($y=0$)	$u=0,\ v=0$	$\frac{\partial T}{\partial y}=0$
Vertical	Left($x=0$)	$u=0,\ v=0$	T_h
	Right $(H-L\le x\le H,\ \frac{H}{2}-\frac{L}{2}\le y\le\frac{H}{2}+\frac{L}{2})$	$u=0,\ v=0$	T_c

The thermophysical properties are listed in Table 2 and boundary conditions in Table 3. For non - dimensionalising equations (4.1) - (4.4), we consider [4,19]

$$X=\frac{x}{H};Y=\frac{y}{H};U=\frac{uH}{\alpha_{bf}};V=\frac{vH}{\alpha_{bf}};P=\frac{pH^2}{\rho_{bf}\alpha_{bf}^2};$$
$$\theta=\frac{T-T_c}{\Delta_T};Ha=B_0H\sqrt{\frac{\sigma_{bf}}{\mu_{bf}}};\ \nu_{bf}=\tfrac{\mu_{bf}}{\rho_{bf}};$$
$$Ra=\tfrac{\beta_{bf}g\Delta TH^3}{\alpha_{bf}\nu_{bf}};Pr=\tfrac{\nu_{bf}}{\alpha_{bf}};$$

then the non dimensionalized equations of $(1)-(4)$ are:

$$\frac{\partial U}{\partial X}+\frac{\partial V}{\partial Y}=0 \tag{4.18}$$

$$\frac{\rho_{\rm hnf}}{\rho_{\rm bf}}\left(U\frac{\partial U}{\partial X}+V\frac{\partial U}{\partial Y}\right)=-\frac{\partial P}{\partial X}+\frac{\mu_{\rm hnf}}{\alpha_{\rm bf}\rho_{\rm bf}}\left(\frac{\partial^2U}{\partial X^2}+\frac{\partial^2U}{\partial Y^2}\right) \tag{4.19}$$

$$\frac{\rho_{\rm hnf}}{\rho_{\rm bf}}\left(U\frac{\partial V}{\partial X}+V\frac{\partial V}{\partial Y}\right)=-\frac{\partial P}{\partial Y}+\frac{\mu_{\rm hnf}}{\alpha_{\rm bf}\rho_{\rm bf}}\left(\frac{\partial^2V}{\partial X^2}+\frac{\partial^2V}{\partial Y^2}\right)+\frac{(\rho\beta)_{\rm hnf}RaPr\theta}{\beta_{\rm bf}\rho_{\rm bf}}-\frac{\sigma_{\rm hnf}}{\sigma_{\rm bf}}Ha^2PrV \tag{4.20}$$

$$U\frac{\partial\theta}{\partial X}+V\frac{\partial\theta}{\partial Y}=\frac{\alpha_{\rm hnf}}{\alpha_{\rm bf}}\left(\frac{\partial^2\theta}{\partial X^2}+\frac{\partial^2\theta}{\partial Y^2}\right) \tag{4.21}$$

The local Nusselt number is $Nu=\dfrac{h(y)H}{\kappa_{bf}}$,

where $h(y)=-\dfrac{\kappa_{hnf}}{\kappa_{bf}\Delta T}\dfrac{\partial T}{\partial x}$ is the heat transfer coefficient.

i.e., $Nu=-\dfrac{\kappa_{hnf}}{\kappa_{bf}\Delta T}H\dfrac{\partial T}{\partial x}$.

On Non -dimensionalising, we get $Nu=-\dfrac{\kappa_{hnf}}{\kappa_{bf}}\dfrac{\partial\theta}{\partial X}$.

And the average Nusselt number is $N\bar{u}=-\dfrac{\kappa_{hnf}}{\kappa_{bf}}\displaystyle\int_0^1\frac{\partial\theta}{\partial X}dY$.

5. Numerical Procedure

The thermal and fluid flow within the C- shaped cavity are analyzed using COMSOL Multiphysics 6.0, a commercial simulation platform known for its ability to handle coupled physics problems. By default the Galerkin Finite Element Method is applied in the software, which is well-suited for solving non - linear PDE problems. For the present investigation, the entire domain is divided into triangular mesh elements. The solution variables are then approximated over this domain using linear shape functions. The resultant mesh topology is presented visually in **Figure 2**. To proceed with the solution, the governing partial differential equations (PDEs), in conjunction with the system-specific boundary conditions detailed in Table 2, are systematically reformulated into their weak (integral) forms. These integrals are subsequently evaluated numerically utilizing the Gaussian Quadrature method, which produces a final, extensive nonlinear algebraic system ready for computational processing. This system is then solved recurrently using the Newton-Raphson method until convergence criteria are satisfied.

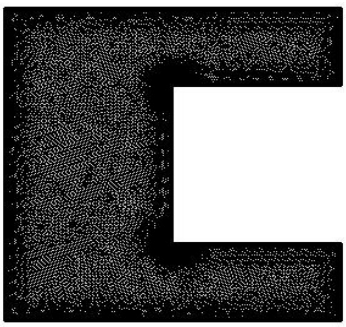

Figure 2: Discretization of computational domain

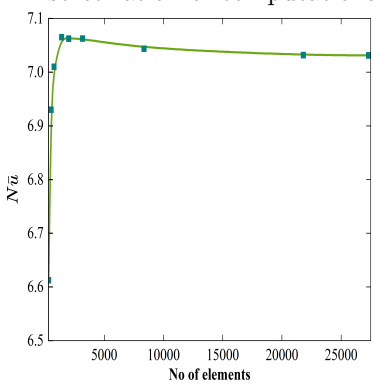

Figure 3: Grid Independence Study

5.1. Grid independence study

To validate the numerical results, a mesh independence analysis is performed by systematically varying the mesh density. This involves altering the number of elements through the selection of mesh types ranging from lower values to extremely fine, as available in the simulation tool. The process is repeated until the $N\bar{u}$ reaches a stable value, showing minimal change with further refinement. This behavior confirms that the solution is no longer influenced by the mesh size. For the conditions $\mathrm{Ra} = 10^6$ and $\phi = 0.04$, as presented in **Figure 3**, the solution stabilizes when the mesh consists of $27,309$ elements. Hence, this mesh is adopted for all subsequent simulations.

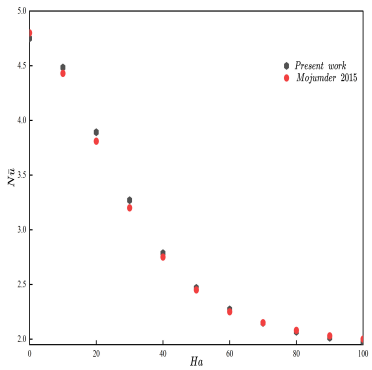

Figure 4: Validation Plot

5.2. Code Validation

Figure 4 presents a comparison between the mean Nusselt number $N\bar{u}$ obtained in the present study and the benchmark results reported by Mojumder [4] for the different Ha. The two sets of data exhibit a consistently close correspondence, with both showing a monotonic decrease in $N\bar{u}$ as Ha increases, reflecting the well-established damping effect of the magnetic field on buoyancy-driven convection. The quantitative agreement across the entire Ha range confirms that the present numerical formulation accurately captures the influence of Lorentz forces on the flow and heat transfer behaviour. This comparison verifies the credibility and robustness of the current computational model for analysing MHD natural convection of hybrid nanofluid in enclosed C-shaped cavity.

6. Result and Discussion

Figure 5 through **figure** 7 present streamline and isotherm distributions for a C-shaped enclosure filled with hybrid nanofluid at a fixed volume fraction of $\phi = 0.03$ and a Rayleigh number of $Ra = 10^4$, with varying Hartmann numbers ($Ha = 0, 50, 100$). In the absence of a magnetic field (Figure 5), the buoyancy-driven flow generates a dominant central vortex with noticeable recirculation, indicating a moderate level of convective heat transfer. As the magnetic field strength increases (Figures 6 and 7), the Lorentz force begins to suppress fluid motion, leading to a reduction in the intensity of circulation. This dampening effect is clearly visible in the more stretched and less curved streamlines, as well as the parallel isotherms indicating conduction-dominant heat transport.

Figure 8 to figure 10 explore the system's response to increased thermal driving force at $Ra = 10^5$, again with $Ha = 0, 50, 100$. A substantial intensification in fluid motion is noticed in Figure 8, where the streamlines display more prominent stronger vortex formations and enhanced flow interaction As Ha increases (Figures 9 and 10), the fluid motion is further suppressed, producing less intense convective structures. Despite this, the flow is still comparatively stronger than in the $Ra = 10^4$ cases, indicating that a higher Rayleigh number partially offsets the magnetic suppression. The isotherms bend more noticeably toward the interior of the cavity in Figure 8, whereas in Figure 10 they appear flatter and nearly parallel to the vertical walls, demonstrating an increased dominance of conduction under stronger magnetic damping.

Figure 11 – figure 13 show that raising Ra to 10^6 intensifies convection, resulting in more irregular streamlines and layered vortex patterns. The temperature field begins to demonstrate sharper gradients near the walls, indicating significant thinning of thermal boundary layers. These effects are most evident when $Ha = 0$ (Figure 11), where the flow is vigorous. However, with $Ha = 50$ and $Ha = 100$ (Figures 12 and 13), the damping influence of the magnetic field again becomes evident, leading to reduced circulation and more parallel isotherms, although not as dominant as in lower Ra cases.

Figure 14 to figure 16 extend the analysis to $Ra = 10^7$. At this elevated Rayleigh number, the system is fully convection-driven when no magnetic field is present (Figure 14). The streamlines show strong, complex vortices indicating intense recirculation. As Ha increases (Figures 15 and 16), suppression

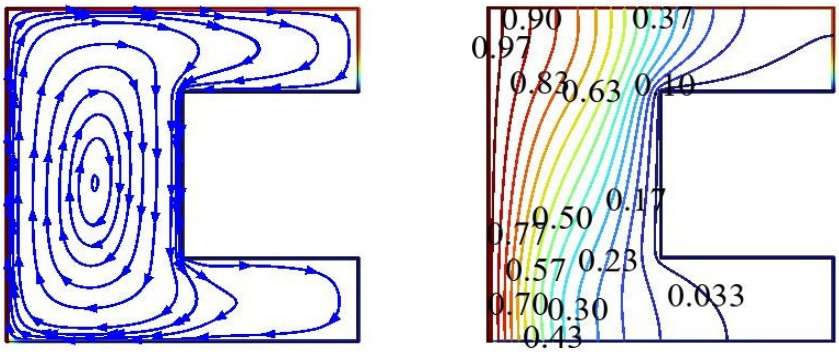

Figure 5: Qualitative visualization of (a) streamlines and (b) isotherms for $Ra = 10^4$, $\phi = 0.03$, and $Ha = 0$.

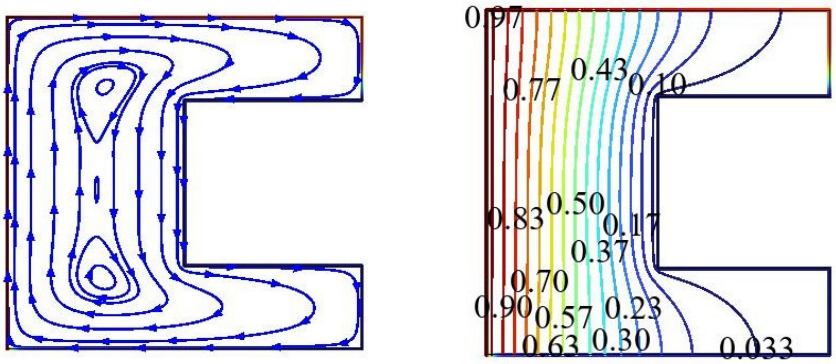

Figure 6: Qualitative visualization of Streamline (a) and Isotherm (b), when $Ra = 10^4$ and $\phi = 0.03$ and $Ha = 50$.

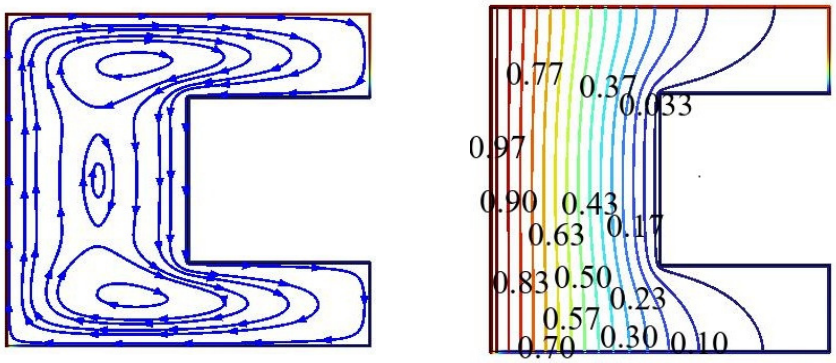

Figure 7: Qualitative visualization of Streamline (a) and Isotherm (b), when $Ra = 10^4$ and $\phi = 0.03$ and $Ha = 100$.

of flow is observed, but due to the very high buoyancy forces, the flow remains considerably strong. The isotherms shift noticeably toward the cold wall, and the thermal gradients are steep near the boundaries. This confirms that, at high Rayleigh numbers, convective heat transfer dominates regardless of magnetic field strength, although the Lorentz force still modulates the flow structure and thermal distribution.

Figure 17 – figure 19 illustrate the effect of aspect ratio AR on the organization of the flow and thermal fields within the cavity. At a lower aspect ratio, the streamlines form broad and well-developed recirculating cells, while the isotherms exhibit strong distortion, confirming the dominance of buoyancy-

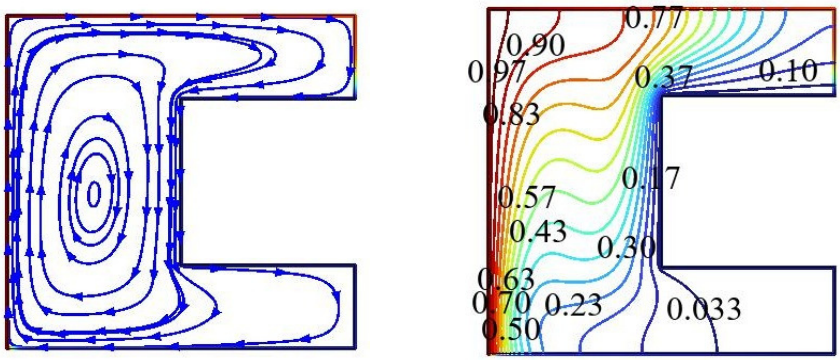

Figure 8: Qualitative visualization of Streamline (a) and Isotherm (b), when $Ra = 10^5$ and $\phi = 0.03$ and $Ha = 0$.

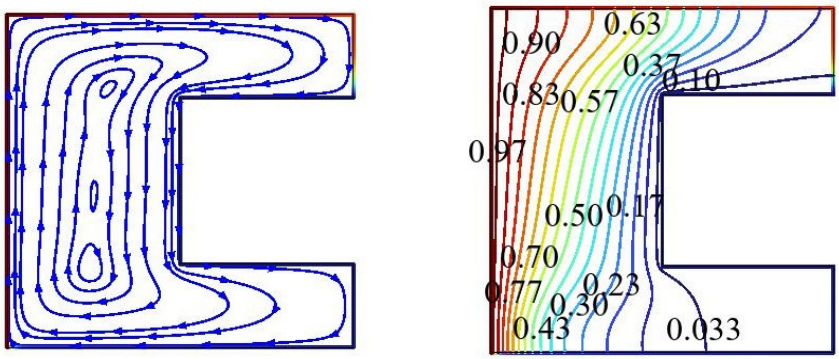

Figure 9: Qualitative visualization of Streamline (a) and Isotherm (b), when $Ra = 10^5$ and $\phi = 0.03$ and $Ha = 50$.

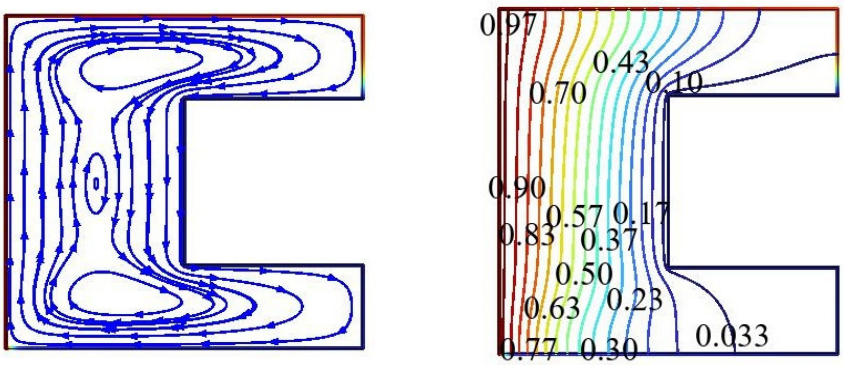

Figure 10: Qualitative visualization of Streamline (a) and Isotherm (b), when $Ra = 10^5$ and $\phi = 0.03$ and $Ha = 100$.

driven convection. As the aspect ratio increases, the flow structure is reorganized into elongated and vertically oriented circulation paths rather than being suppressed. This geometric confinement leads to steeper temperature gradients near the heated wall, indicating sustained and directional convective heat transfer even under magnetic field influence. The observed changes demonstrate that the aspect ratio primarily modifies the flow topology and thermal transport pathways, thereby playing a significant role in governing the overall heat transfer behavior of the hybrid nanofluid.

Figure 20 illustrates the dependence of the mean Nusselt number on the Hartmann number for

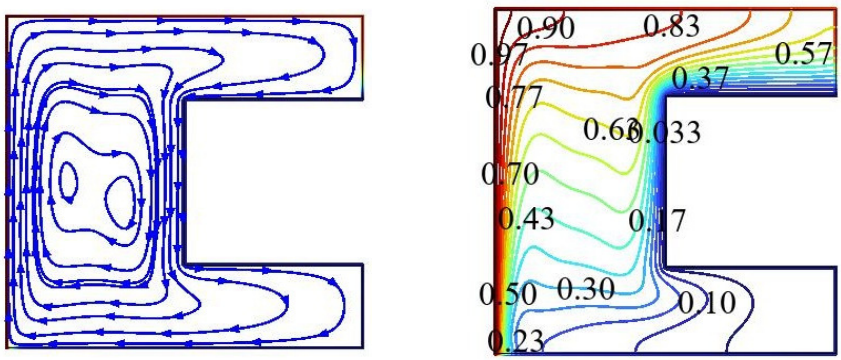

Figure 11: Qualitative visualization of Streamline (a) and Isotherm (b), when $Ra = 10^6$ and $\phi = 0.03$ and $Ha = 0$.

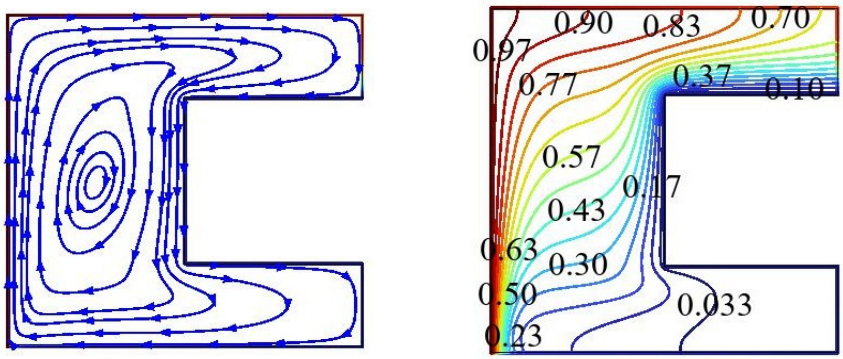

Figure 12: Qualitative visualization of Streamline (a) and Isotherm (b), when $Ra = 10^6$ and $\phi = 0.03$ and $Ha = 50$.

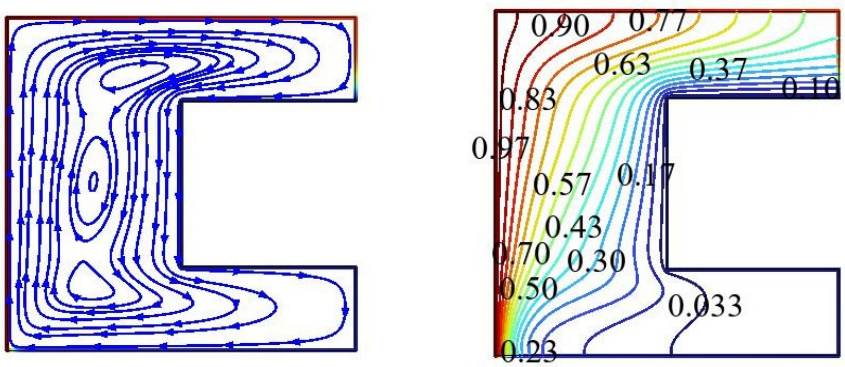

Figure 13: Qualitative visualization of Streamline (a) and Isotherm (b), when $Ra = 10^6$ and $\phi = 0.03$ and $Ha = 100$.

different Rayleigh numbers. As expected, $N\bar{u}$ increases with increasing Ra, reflecting the enhancement of buoyancy forces and the resulting intensification of natural convection. Higher Rayleigh numbers promote stronger flow circulation and more effective heat transport from the heated to the cooled boundary. In contrast, $N\bar{u}$ decreases with increasing Ha, particularly in the low-to-moderate magnetic field range ($Ha = 0$–100). This reduction is associated with the action of the Lorentz force, which suppresses fluid motion, attenuates convective activity, and consequently limits heat transfer.

Figure 21 presents the variation of $N\bar{u}$ with Ra for different Hartmann numbers and shows that,

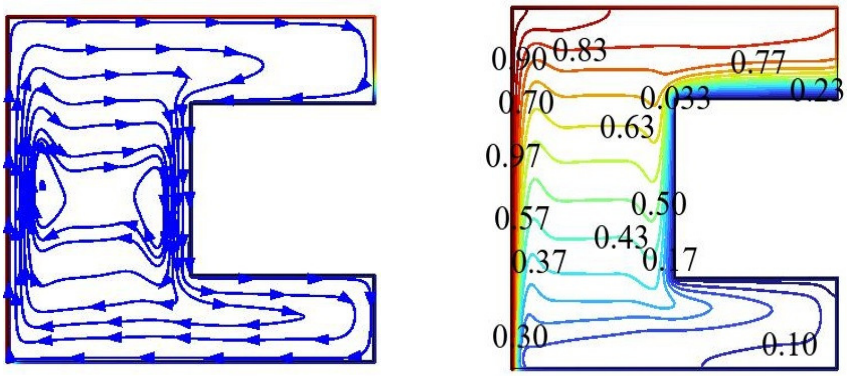

Figure 14: Qualitative visualization of Streamline (a) and Isotherm (b), when $Ra = 10^7$ and $\phi = 0.03$ and $Ha = 0$.

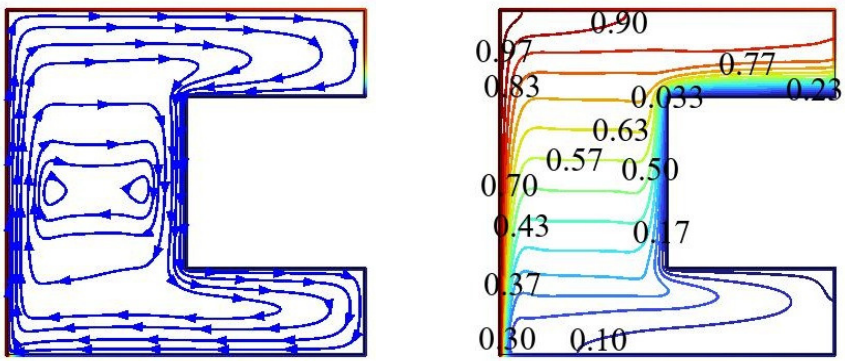

Figure 15: Qualitative visualization of Streamline (a) and Isotherm (b), when $Ra = 10^7$ and $\phi = 0.03$ and $Ha = 50$.

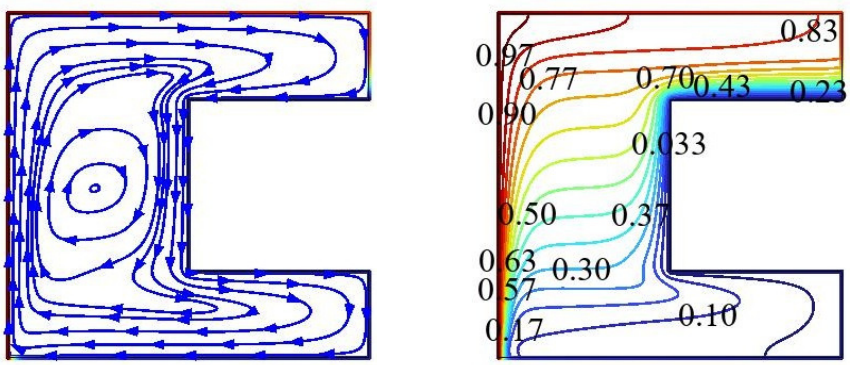

Figure 16: Qualitative visualization of Streamline (a) and Isotherm (b), when $Ra = 10^7$ and $\phi = 0.03$ and $Ha = 100$.

for any given Ra, increasing Ha consistently reduces heat transfer. This behaviour further confirms that a stronger magnetic field impedes convective motion and lowers thermal transport effectiveness. The influence of Ha becomes more pronounced at larger Rayleigh numbers, where convection is dominant in the absence of a magnetic field but becomes noticeably weakened under magnetic damping.

Figure 22 depicts the variation of $N\bar{u}$ with Ra for different nanoparticle volume fractions ($1\% \leq \phi_{np} \leq 4\%$). As both ϕ_{np} and Ra increase, $N\bar{u}$ also increases. The enhancement in heat transfer is due

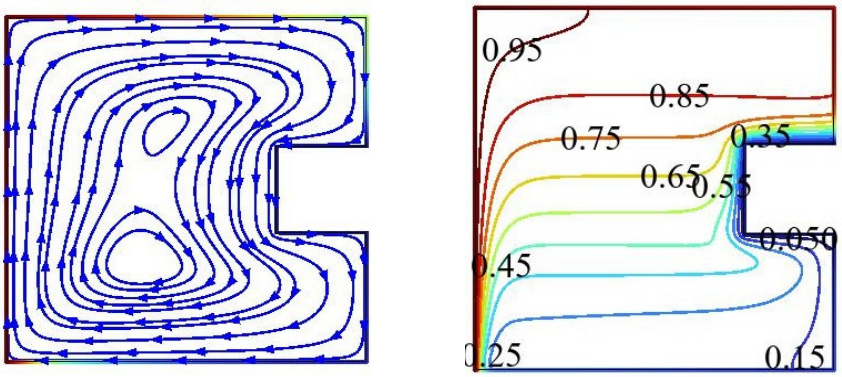

Figure 17: Qualitative visualization of Streamline (a) and Isotherm (b) at $AR = 0.25$ $Ra = 10^5$, $\phi = 0.03$, and $Ha = 50$.

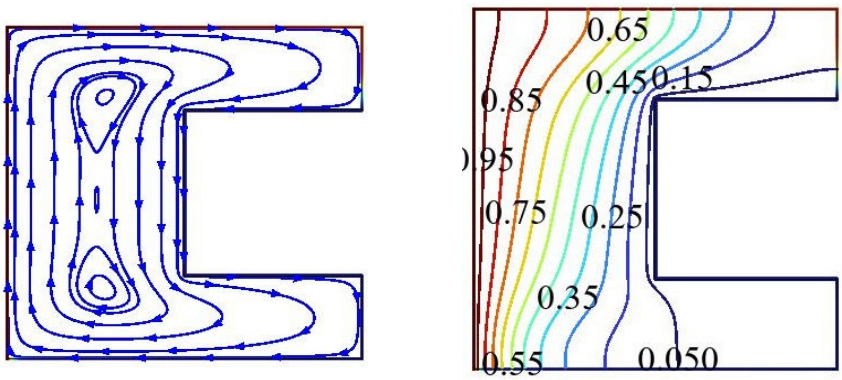

Figure 18: Qualitative visualization of Streamline (a) and Isotherm (b) at $AR = 0.50$ $Ra = 10^5$, $\phi = 0.03$, and $Ha = 50$.

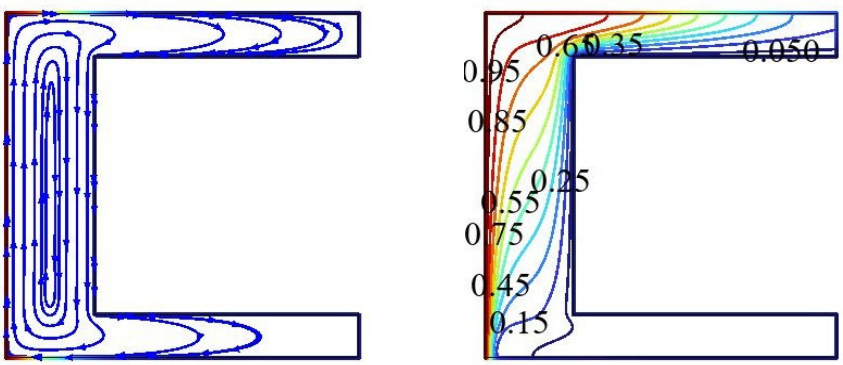

Figure 19: Qualitative visualization of Streamline (a) and Isotherm (b) at $AR = 0.75$ $Ra = 10^5$, $\phi = 0.03$, and $Ha = 50$.

to the improved thermal conductivity of the nanofluid with increasing nanoparticle concentration. The improvement in the fluid's effective thermal conductivity boosts convective heat transfer, which in turn raises the Nusselt number.

Figure 23 depicts the variation of the $N\bar{u}$ with the Ra for different ϕ_{np}. It can be observed that the $N\bar{u}$ increases steadily as the Ra increases for all values of ϕ_{np}, signifying the transition toward stronger natural convection due to enhanced buoyancy effects. In addition, for a given Ra, higher ϕ_{np} result in larger Nusselt numbers, demonstrating improved heat transfer characteristics of the nanofluid. This

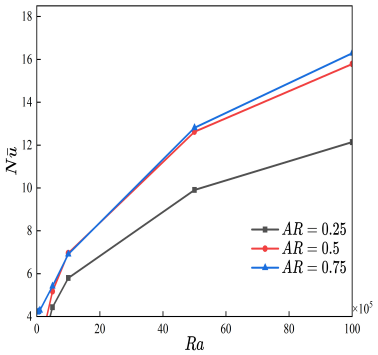

Figure 20: Quantitative plot of $N\bar{u}$ vs Ra for different AR values

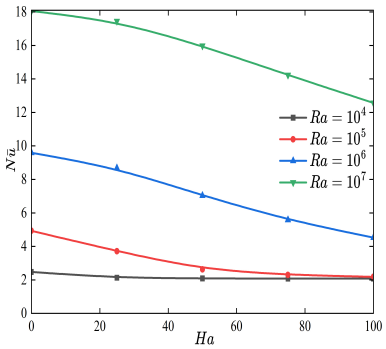

Figure 21: Quantitative plot of the $N\bar{u}$ vs Ha for different Ra at fixed $\phi = 0.03$.

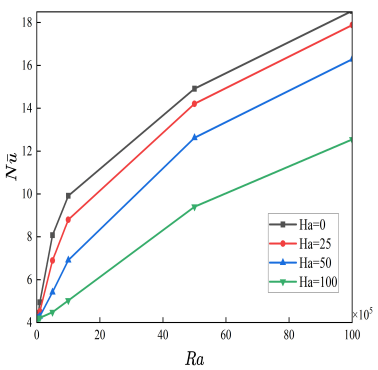

Figure 22: Quantitative plot of $N\bar{u}$ vs Ra for the distinct value of Ha with $\phi = 0.03$.

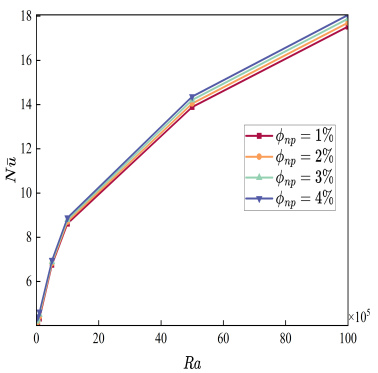

Figure 23: Quantitative plot of $N\bar{u}$ vs Ra for the distinct value of ϕ with $Ha = 25$.

enhancement arises from the increase in effective thermal conductivity and thermal energy transport caused by the presence of nanoparticles, which strengthens convective heat transfer within the enclosure.

7. Conclusion

A comprehensive numerical investigation has been performed on steady, laminar magnetohydrodynamic (MHD) natural convection of a water-based hybrid nanofluid containing single-walled and multi-walled carbon nanotubes (SWCNTs and MWCNTs) inside a C-shaped enclosure. The governing equations were solved using the Galerkin Finite Element Method, and both qualitative and quantitative analyses were conducted. The flow and temperature characteristics were examined through streamlines and isotherms, while the average Nusselt number ($N\bar{u}$) was used as the primary mode for evaluating heat transfer performance.

The effects of key parameters were explored over wide ranges, namely: aspect ratio ($0.25 \leq AR \leq 0.75$), Rayleigh number ($10^4 \leq Ra \leq 10^7$), Hartmann number ($0 \leq Ha \leq 100$), and hybrid nanoparticle volume fraction ($1\% \leq \phi_{np} \leq 4\%$). The principal findings of the study are summarized below:

- At low Ra, the heat transfer mechanism is predominantly conduction-driven, and the introduction of a magnetic field further reinforces this behavior.
- Increasing Ra or ϕ_{np}, there is an improvement in $N\bar{u}$ due to stronger buoyancy-fluid motion and improved effective thermal conductivity.
- Higher Ha values suppress convective circulation through Lorentz forces, which diminishes the overall heat transfer. This magnetic damping effect becomes less influential at large Ra, where convection remains dominant.
- The case with a lower aspect ratio ($AR = 0.25$) exhibits stronger recirculating motion, which promotes enhanced fluid mixing and supports effective convective heat transfer within the enclosure.
- An increase in the aspect ratio alters the cavity geometry such that buoyancy-driven flow is redirected into elongated pathways rather than being suppressed, leading to intensified temperature gradients near the heated surfaces and sustained convective heat transport even in the presence of magnetic damping.

Acknowledgments

We gratefully acknowledge the software support provided by the I-STEM program, funded by the Office of the Principal Scientific Adviser to the Government of India. This support facilitated the research conducted at the Nitte Meenakshi Institute of Technology using facilities registered and reserved through the I-STEM web portal.

References

1. Mostafa Mahmoodi, Seyed Mohammad Hashemi, Numerical study of natural convection of a nanofluid in C-shaped enclosures, International Journal of Thermal Sciences, 55 (2012) 76-89.
2. M.A. Mansour, M.A. Bakeir, A. Chamkha, Natural convection inside a C-shaped nanofluid-filled enclosure with localized heat sources, International Journal of Numerical Methods for Heat & Fluid Flow, Vol. 24 No. 8, 2014 pp. 1954-1978.
3. M.A.Y. Bakier, Flow in open C-shaped cavities: How far does the change in boundaries affect nanofluid?, Engineering Science and Technology, an International Journal 17 (2014) 116-130.
4. Satyajit Mojumder, Sourav Saha, Sumon Saha, M.A.H. Mamun, Effect of magnetic field on natural convection in a C-shaped cavity filled with ferrofluid, 6th BSME International Conference on Thermal Engineering (ICTE 2014).
5. N. Makulati, A. Kasaeipoor, M.M. Rashidi, Numerical study of natural convection of a water–alumina nanofluid in inclined C-shaped enclosures under the effect of magnetic field, Advanced Powder Technology, APT 1185 (2016).
6. Rasul Mohebbi, Mohsen Izadi and Ali J. Chamkha, Heat source location and natural convection in a C-shaped enclosure saturated by a nanofluid, PHYSICS OF FLUIDS 29, 122009 (2017).
7. Mohsen Izadi, Rasul Mohebbi, A. Chamkha, Ioan Pop, Effects of cavity and heat source aspect ratios on natural convection of a nanofluid in a C-shaped cavity using Lattice Boltzmann method, International Journal of Numerical Methods for Heat & Fluid Flow © Emerald Publishing Limited, 2018, 0961-5539.

8. Mohammad Hemmat Esfe, Ali Akbar Abbasian Arani, Wei-Mon Yan, Hamidreza Ehteram, Alireza Aghaie, Masoud Afrand, Natural convection in a trapezoidal enclosure filled with carbon nanotube–EG–water nanofluid, International Journal of Heat and Mass Transfer 92 (2016) 76–82.

9. Amin Matori, Rasul Mohebbi, Zahra Hashemi, Yuan Ma, Lattice Boltzmann study of multi-walled carbon nanotube $(MWCNT) - Fe_3O_4$/water hybrid nanofluids natural convection heat transfer in a π shaped cavity equipped by hot obstacle, Journal of Thermal Analysis and Calorimetry (2019) 136:2495–2508.

10. Dwesh K. Singh, Free convection with MWCNT/water nanofluid having varying aspect ratio of MWCNT nanoparticle in thermally undulated enclosures, International Journal of Mechanical Sciences 178 (2020) 105626.

11. Reza Sarlak, Azher M. Abed, Omid Ali Akbari, Ali Marzban, Shaghayegh Baghaei, Mohammad Bayat, Numerical investigation of natural convection heat transfer of water/ SWCNT nanofluid flow in a triangular cavity with cold fluid injection, Progress in Nuclear Energy 155 (2023) 104513.

12. Mohsen Izadi, Rasul Mohebbi, Davood Karimi, Mikhail A. Sheremet, Numerical Simulation of Natural Convection Heat Transfer inside a $\perp$ Shaped Cavity Filled by a $MWCNT - Fe_3O_4$/Water Hybrid Nanofluids using LBM, Chemical Engineering and Processing, 2018.

13. Pranit Joshi, Arvind Pattamatta, An experimental study on buoyancy induced convective heat transfer in a square cavity using multi-walled carbon nanotube (MWCNT)/water nanofluid, 7th European Thermal-Sciences Conference (Eurotherm 2016, Journal of Physics: Conference Series 745 (2016).

14. Patrice Estelle, Omid Mahian, Thierry Mare, Hakan F. Oztop, Natural convection of CNT water-based nanofluids in a differentially heated square cavity, J Therm Anal Calorim (2017) 128:1765–1770.

15. Rizwan Ul Haq, Feroz Ahmed Soomro, Z. Hammouch, Sajjad Ur Rehman, Heat exchange within the partially heated C-shape cavity filled with the water based SWCNTs, International Journal of Heat and Mass Transfer 127 (2018) 506–514.

16. M. Hamid, Z. H. Khan, W. A. Khan, and R. U. Haq, Natural convection of water-based carbon nanotubes in a partially heated rectangular fin-shaped cavity with an inner cylindrical obstacle, Phys. Fluids 31, 103607 (2019).

17. Desh Deepak Dixit and Arvind Pattamatta, Natural convection heat transfer in a cavity filled with electrically conducting nano-particle suspension in the presence of magnetic field, Phys. Fluids 31, 023302 (2019).

18. Rizwan Ul Haq, Syed Saqib Shah, Ebrahem A. Algehyne, Iskander Tlili, Heat transfer analysis of water based SWCNTs through parallel fins enclosed by square cavity, International Communications in Heat and Mass Transfer 119 (2020) 104797

19. Oktay Cicek, Mikhail A. Sheremet, A. Cihat Baytas, Effect of natural convection hybrid nanofluid flow on the migration and deposition of $MWCNT-Fe_3O_4$ in a square enclosure, International Journal of Thermal Sciences 190 (2023) 108318.

20. Fatih Selimefendigil and Hakan F. Öztop, Natural convection and melting of NEPCM in a corrugated cavity under the effect of magnetic field, Journal of Thermal Analysis and Calorimetry (2020) 140:1427–1442.

21. Sardar Bilal, Imtiaz Ali Shah, Kaouther Ghachem, Abdelkarim Aydi and Lioua Kolsi, Heat Transfer Enhancement of MHD Natural Convection in a Star-Shaped Enclosure, Using Heated Baffle and MWCNT–Water Nanofluid, Mathematics 2023, 11, 1849.

22. T.O. Scott, D.R.E. Ewim, A.C. Eloka-Eboka, Experimental study on the influence of volume concentration on natural, convection heat transfer with Al_2O_3MWCNT/water hybrid nanofluids,Materials Today: Proceedings 105 (2024) 78–84.

23. Rizwan Ul Haq, Feroz Ahmed Soomro, Hakan F. Öztop, Toufik Mekkaoui, Thermal management of water-based carbon nanotubes enclosed in a partially heated triangular cavity with heated cylindrical obstacle, International Journal of Heat and Mass Transfer 131 (2019) 724–736.

24. Zafar H. Khan, Waqar A. Khan, R.U. Haq, M. Usmand, M. Hamid, Effects of volume fraction on water-based carbon nanotubes flow in a right- angle trapezoidal cavity: FEM based analysis, International Communications in Heat and Mass Transfer 116 (2020) 104640.

25. L.Th. Benos, E.G. Karvelas, I.E. Sarris, Crucial effect of aggregations in CNT-water nanofluid magnetohydrodynamic natural convection, Thermal Science and Engineering Progress 11 (2019) 263–271.

26. Eid S. Alatawi, Enhancing Heat Transfer Efficiency Through Controlled Magnetic Flux in a Partially Heated Circular Cavity Using Multi-Walled Carbon Nanotube Nanofluid and an Internal Square Body, Sustainability 2024, 16, 10632.

27. Rizwan Ul Haq, S. Naveed Kazmi, Toufik Mekkaoui, Thermal management of water based SWCNTs enclosed in a partially heated trapezoidal cavity via FEM, International Journal of Heat and Mass Transfer 112 (2017) 972–982.

28. Yuan Ma, Rasul Mohebbi, Mohammad Mehdi Rashidi, Zhigang Yang, Effect of hot obstacle position on natural convection heat transfer of MWCNTs-water nanofluid in U-shaped enclosure using lattice Boltzmann method, International Journal of numerical Methods for Heat & Fluid Flow © Emerald Publishing Limited, 0961-5539 (2018).

29. Djellouli Ghali, Fares Redouane, Roubi Abdelhak, Amine Belhadj Mahammed, Chikr Djaoutsi Zineb, Wasim Jamshed, Mohamed R. Eid, Sayed M. Eldin, Awad Musa and Nor Ain Azeany Mohd Nasir, Mathematical Entropy Analysis of Natural Convection of $MWCNT|Fe_3O_4$/Water Hybrid Nanofluid with Parallel Magnetic Field via Galerkin Finite Element Process, Symmetry 2022, 14, 2312.

30. Zafar H. Khana, Waqar A. Khanb, R.U. Haq, M. Usmand, M. Hamid, Effects of volume fraction on water-based carbon nanotubes flow in a right- angle trapezoidal cavity: FEM based analysis, International Communications in Heat and Mass Transfer 116 (2020) 104640.

31. G. R. Manohar, P. Venkatesh, B. J. Gireeshaa, J. K. Madhukesh and G. K. Ramesh, Performance of water, ethylene glycol, engine oil conveying SWCNT-MWCNT nanoparticles over a cylindrical fin subject to magnetic field and heat generation, INTERNATIONAL JOURNAL OF MODELLING AND SIMULATION 2022, VOL. 42, NO. 6, 936–945.

Pramod S.,
Department of Mathematics,
Nitte Meenakshi Institute of Technology (NMIT), Bengaluru, Nitte (Deemed to be University), India.
Department of Mathematics,
B.M. S. College of Engineering, Bengaluru–560019.
Visvesvaraya Technological University, Belagavi, Karnataka, India.
E-mail address: praup.s@gmail.com

and

Sujatha N.,
Department of Mathematics,
B.M. S. College of Engineering, Bengaluru–560019.
Visvesvaraya Technological University, Belagavi, Karnataka, India.
E-mail address: sujathan.maths@bmsce.ac.in

and

Sreekala C. K.,
Department of Mathematics,
Nitte Meenakshi Institute of Technology (NMIT), Bengaluru, Nitte (Deemed to be University), India.
E-mail address: sreekalarajeesh@gmail.com